Chapter 4
Coupled DIC and IRT Analysis of Strain Rate and Temperature Effects on Aluminum Alloy Fracture

D. Zeng, Z. Li, A. Leonard, T. Schmidt, C. Giesige, J. Carrock, and J. Gardiner

Abstract Aluminum alloys, traditionally considered a strain-rate insensitive material, have recently demonstrated an unexpected increase in fracture strain at elevated strain rates. This phenomenon has significant implications for automotive crashworthiness, particularly given the increasing usage of aluminum in vehicle body structures. Accurate fracture modeling for these simulations requires high-fidelity inputs, making the characterization of fracture strain under varying rates a critical parameter.

This paper presents a novel methodology coupling Digital Image Correlation (DIC) and high-speed Infrared Thermography (IRT) for characterizing the fracture behavior of aluminum alloys under high speed testing. The experimental setup utilizes precise system triggering and temporal verification to synchronize thermal data with deformation fields. By mapping temperature changes directly onto deformation fields, the system enables the spatial alignment of thermal maps and surface strain distributions, effectively capturing the material's thermo-mechanical progression. The resulting data quantifies the relationship between adiabatic heating and fracture sensitivity, enabling a precise evaluation of thermal softening effects. Ultimately, this work provides the essential quantitative evidence needed to refine fracture criteria for advanced aluminum alloys and validated inputs for crash simulation models.

Keywords Digital Image Correlation · thermography · Strain

Introduction

Aluminum alloys are extensively utilized in automotive structural components due to their high strength-to-weight ratio. With the increasing applications of aluminum for lightweight vehicle body design, there has been a significant rise in comprehensive studies characterizing these materials. While strain rate sensitivity is a critical parameter, conventional understanding suggests that aluminum is either rate-insensitive or exhibits negative rate sensitivity [1, 2], leaving the effects on fracture strain largely unexplored.

However, our recent experimental data from material tests reveal a critical deviation from this convention: fracture strain increases significantly with strain rate. Specifically, at strain rates of 500 to1000/s and above, the fracture strain can be more than doubled. This phenomenon is likely caused by adiabatic heating. As the material plastic deformation increases, plastic work is converted into heat. During high-speed testing, the short duration prevents this heat from dissipating, leading to a localized temperature rise. As we know, thermal softening will result in elevated fracture strain that differs significantly from quasi-static room temperature behavior. In this study, a coupled optical approach is developed to investigate the relationship between strain rate and temperature rise.

D. Zeng · Z. Li
Ford Motor Company, 2101 Village Road, Dearborn, MI, 48121, USA
e-mail: dzeng@ford.com;zli75@ford.com

A. Leonard · T. Schmidt
Trilion Quality Systems, 651 Park Ave, King of Prussia, PA 19406, USA
e-mail: AndyL@trilion.com;Schmidt@trilion.com

Giesige · J. Carrock · J. Gardiner
Telops, 100-2600 Avenue St.-Jean-Baptiste, Québec (Québec), Canada G2E 6J5
e-mail: c.giesige@exosens.com;j.carrock@exosens.com; j.gardiner@exosens.com

© The Author(s), under exclusive license to River Publishers 2026

Motoharu Fujigaki et al. (eds.), *Advancement of Optical Methods & Digital Image Correlation in Experimental Mechanics, Volume 2, 2026*, Conference Proceedings of the Society for Experimental Mechanics Series, https://doi.org/10.13052/rp-9788743816256

Digital Image Correlation (DIC) has established itself as the premier non-contact optical method for local displacement and strain measurement, gaining widespread applications due to its versatility and high fidelity in characterizing material deformation fields [4, 5]. This technique enables the generation of full-field displacement and strain maps by tracking stochastic patterns across a series of images captured during material deformation. The method has been significantly enhanced by the development of robust commercial platforms (most notably the Zeiss ARAMIS system), which have become a standard for complex material and component testing in the automotive and aerospace sectors [6, 7]. These advanced systems allow for precise measurements even under challenging conditions; for instance, Xie [8] utilized a multi-camera setup to capture extreme large deformations in soft polymers.

While DIC provides a comprehensive kinematic description, it remains blind to the thermal state of the materials. Infrared (IR) thermography complements DIC by providing non-contact, full-field temperature measurements. However, capturing the transient thermal phenomena inherent in high-strain-rate fracture requires extreme temporal resolution. In this field, state-of-the-art high-speed IR cameras, such as those developed by Telops, address this challenge. These systems utilize high-performance Indium Antimonide (InSb) or Mercury Cadmium Telluride (MCT) detectors capable of capturing thermal fields at tens of thousands of frames per second with microsecond integration times [9]. This capability is critical for 'freezing' the motion of rapidly deforming specimens and accurately resolving the adiabatic heating generated during catastrophic failure [11, 12].

Synchronizing high-speed IRT with DIC allows for capturing the complex thermo-mechanical interactions during material failure. This combination is critical for revealing the coupling effect during loading such as capturing thermoelastic response and heat generation, where thermal strain at each data point can be calculated and subtracted leaving only the mechanical strain response [13]. However, in dynamic material characterization, these events evolve on microsecond timescales. Standard frame-rate systems often suffer from temporal aliasing, failing to capture the peak adiabatic temperature rise within the localized deformation zone. Consequently, a synchronized high-speed framework is essential to ensure that the rapid evolution of strain localization is temporally resolved and spatially aligned.

This paper presents an integrated framework for high-strain-rate tensile fracture characterization using the synchronized high speed DIC and IRT. The proposed acquisition workflow employs precise triggering to align thermal maps with surface strain fields, enabling the extraction of coupled thermo-mechanical behavior. To validate this methodology, tensile tests are conducted on two aluminum alloys, including a 5xxx-series sheet and a cast aluminum alloy. Additionally, quasi-static tests are performed to establish a baseline for rate sensitivity. Beyond the experimental results, this paper provides practical guidance on optical setup such as camera placement, field-of-view optimization, frame rate selection, etc. Ultimately, this study demonstrates that integrating DIC with calibrated IR imaging yields a robust diagnostic tool, providing the quantitative evidence necessary to characterize the progression of fracture in lightweight automotive materials.

Experimental Procedures: Coupled DIC and IRT for High-Speed Tensile Tests

Tensile test frame and specimen

High-speed tensile tests were conducted using an MTS servo-hydraulic testing frame. The system can achieve actuator velocities up to 10 m/s, allowing for strain rates ranging from 1 to 1000/s. Specimens were machined into a dog-bone geometry with a gauge length of $10\ \mathrm{mm}$ and a width of $5\ \mathrm{mm}$. Wired EDM was used to ensure high edge quality. Two materials were tested: a 1.5mm thick 5xxx-series aluminum sheet and a 3mm thick cast aluminum plaque.

To minimize inertial ringing and ensure a constant strain rate, a slack-adapter assembly was employed. As shown in Fig. 1, specimens were mounted using lightweight shoulder grips designed to prevent slippage and expedite specimen exchange. Force was measured using a 20kN load cell, while strain was captured via an Aramis DIC system equipped with two high-speed cameras. Additionally, temperature evolution was recorded using a high-speed thermal camera. Speckle patterns are applied on the test specimen for both DIC and IRT. Fig. 2 illustrates the placement of the DIC and IRT systems. The IR camera was positioned in the same plane as the DIC cameras to ensure a shared field of view on the specimen surface.

High speed DIC system

DIC image acquisition was performed using two Photron FASTCAM NOVA S12 high-speed cameras. These units feature a 1-megapixel CMOS sensor capable of recording at 128,000 fps at full resolution (and up to 1,000,000 fps at reduced resolution) with 128GB of internal memory. Illumination was provided by two GS Vitec high-power LED units. The cameras were equipped with Nikon 105 mm macro lenses, and the entire assembly was mounted on a customized heavy-duty tripod. For this experiment, images were acquired at a frame rate of 50,000 fps with a reduced resolution of 512x384 pixels providing



Fig. 1 Test specimen with lightweight shoulder load fixture.



Fig. 2 Illustration of the coupling of DIC and IRT systems.

the necessary temporal resolution to capture deformation at high strain rates. A shutter time of 1/150,000 s was selected to ensure appropriate exposure.

High speed IRT

High-speed thermal imaging was performed using a Telops FAST M3k mid-wave infrared (MWIR) camera. This system features a 320×256 pixel sensor with a maximum frame rate of 3,100 fps at full resolution, and can achieve speeds up to 100,000 fps in subwindow mode. The camera covers a temperature range of 0 to 1500 °C, divided into four calibration bands.

Achieving higher frame rates requires reducing the window size and exposure time. While window size is constrained by specimen geometry, exposure time directly determines the effective dynamic temperature range. Figure 3(a) illustrates the relationship between radiometric temperature and exposure time for the first calibration range (0 to 169°C).

From Fig. 3(a), an exposure time of 20 μs limits the upper measurable temperature to 140°C; As shown in Fig. 3(b), temperature at locations exceeding this value will saturate, indicated by a green 'SAT' overlay. Reducing the exposure time to 10μs in Fig. 3(c) allows temperatures measured above 140°C up to upper detection limit, but it also raises the lower detection limit to 40°C. The 'OCR' label in Fig. 3(c) marks areas where the temperature exceeds the absolute upper bound of the calibration range (169°C), requiring a switch to a higher calibration band.

For this study, the sensor window was reduced to 64x192 pixels to match the aspect ratio of the specimen's gauge section. The camera operated at 10,000 fps with an exposure time of 13μs, providing the necessary temporal resolution to capture rapid temperature changes during high-speed deformation.

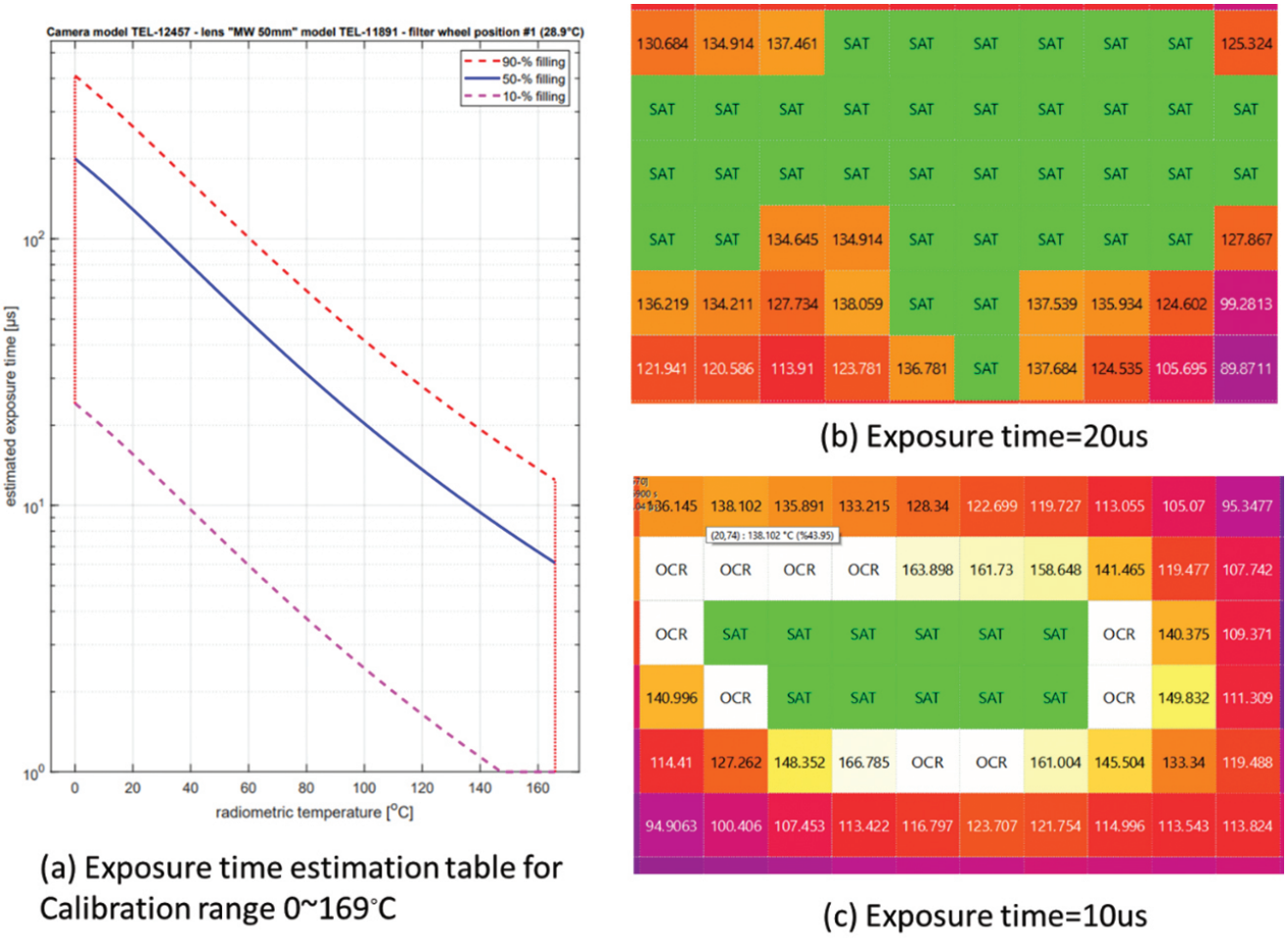

Fig. 3 Estimation of exposure time.

Signal synchronization

Synchronization between mechanical deformation and thermal fields was achieved through a hardware-based master-slave configuration. To ensure precise temporal alignment, a cascaded triggering scheme was implemented: the load frame served as the master source, transmitting a trigger signal to the DIC system before actuator moves. The master camera of the DIC system then immediately relayed a synchronized 5V TTL (Transistor–Transistor Logic) pulse to trigger the infrared camera.

The DIC system recorded at a frame rate five times of the IR camera ($50,000$ fps vs. $10,000$ fps). This setup established a common time-zero and eliminated timing jitter, ensuring the two datasets remained temporally locked. Consequently,

the thermal images could be directly mapped onto the displacement fields, allowing for a pixel-to-pixel correlation of strain and temperature evolution throughout the event.

Data processing

Typically, the Zeiss Quality Suite manages both acquisition and data processing for the Aramis DIC system. However, as high-speed data acquisition is not currently integrated into this platform, the Photron FASTCAM Viewer (PFV4) software was used to control the high-speed cameras. To ensure accuracy, the system calibration followed the standard Aramis protocols, with calibration images captured via PFV4. These images were imported into the Zeiss Quality Suite to compute displacement and strain fields. Since the optical configuration remained unchanged between calibration and testing, the calibration parameters were valid for the post-processing of the imported images.

Thermal data sequences were acquired using Telops Reveal IR, a control software for the FAST M3k camera. However, this software provides thermography maps in a fixed frame of reference and can not specify material points undergoing deformation. To address this, two plugins developed by Trilion Quality Systems were utilized within the Zeiss Quality Suite to synchronize the thermal and mechanical fields.

First, the 'Data Frequency Matcher' algorithm temporally interpolate the thermal sequence to match the exact DIC timestamps. Subsequently, the 'Map Thermography Data' plugin projected the temperature field onto the deformed surface mesh generated by the DIC system. Figure 4 illustrates this integration: Fig. 4(a) shows the raw thermograph from Reveal IR, Fig. 4(b) displays the temperature field mapped onto the DIC geometry, and Fig. 4(c) presents the corresponding strain field. This spatial mapping successfully enables the precise extraction of temperature-strain histories for a specific material point, as demonstrated in Fig. 5.

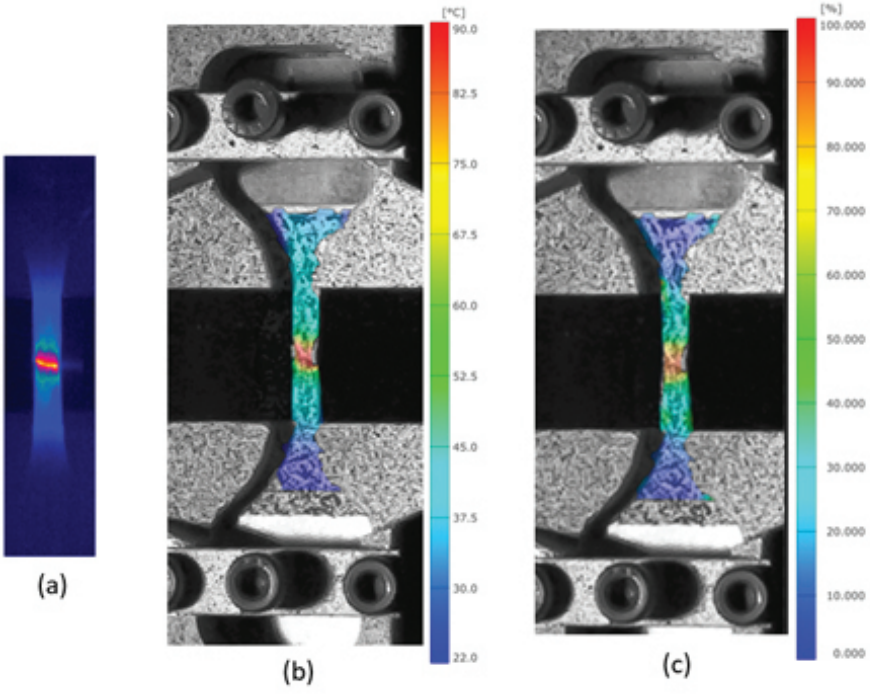

Fig. 4 Synchronization of DIC and IRT results.

Results and Discussion

Following the coupled DIC-IRT framework established in Section 2, this section evaluates two aluminum variants: a 5xxx-series sheet and a cast aluminum alloy. The study focuses on characterizing fracture performance at high strain rates, specifically, examining how adiabatic heating influences fracture behavior during rapid deformation across different manufacturing processes.

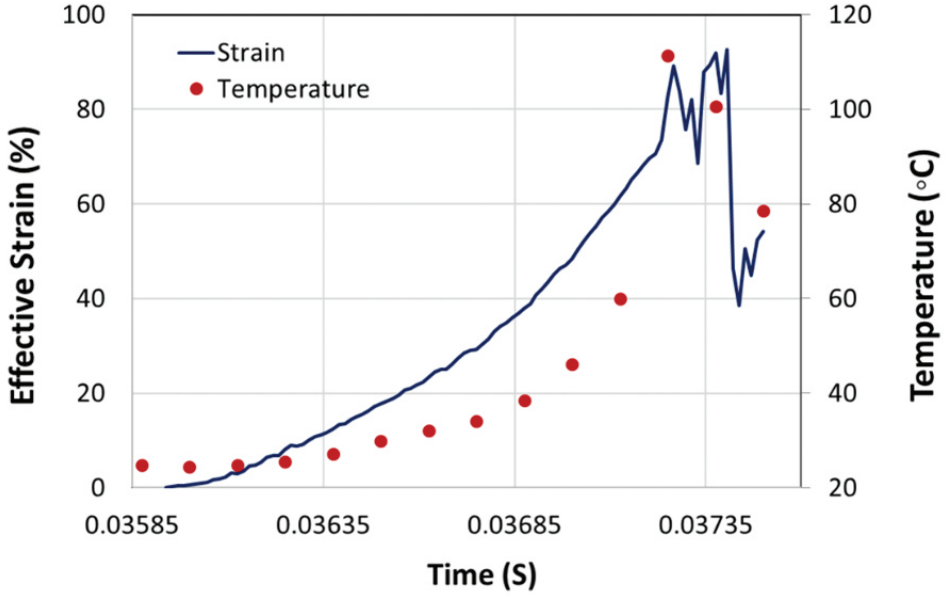

Fig. 5 Strain and temperature evolution during a high-speed test.

Results for 5xxx-series aluminum sheets

5xxx series aluminum is a relatively ductile material. Figure 6 illustrates the evolution of effective strain and the corresponding strain rate at the specimen center during a quasi-static room temperature tensile test. To ensure a valid comparison with the high strain rate data (acquired at a 512x384 pixel resolution), the post-processing parameters for the quasi-static images (12M DIC system, 3000x4000 pixels) were carefully adjusted. Specifically, the facet and step sizes were selected to yield a physical grid size of approximately 0.5 mm, matching the spatial resolution of the high-rate tests.

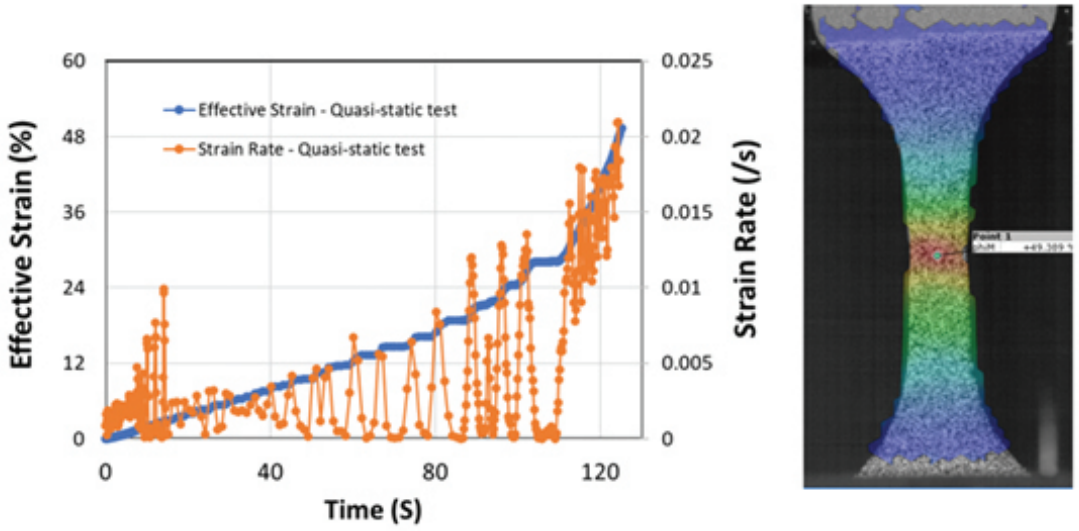

Fig. 6 Evolution of effective strain and strain rate during quasi-static tensile testing of 5xxx-series aluminum at room temperature.

In the quasi-static test (2 mm/min), the localized fracture strain reached 50%, while the strain rate remained below 0.1/s even approaching fracture. The data exhibits significant oscillations in both strain and strain rate, indicating strong serration effect, a phenomenon typical of 5xxx-series aluminum.

Figure 7 presents the results of the same test performed at a high speed of 2m/s. Beyond 25% strain—the limit of uniform elongation—localized necking develops rapidly. Consequently, both strain rate and temperature increase significantly. The temperature exceeded 100°C at failure, with a localized fracture strain of 75%. This represents a significant increase in ductility compared to the quasi-static baseline.

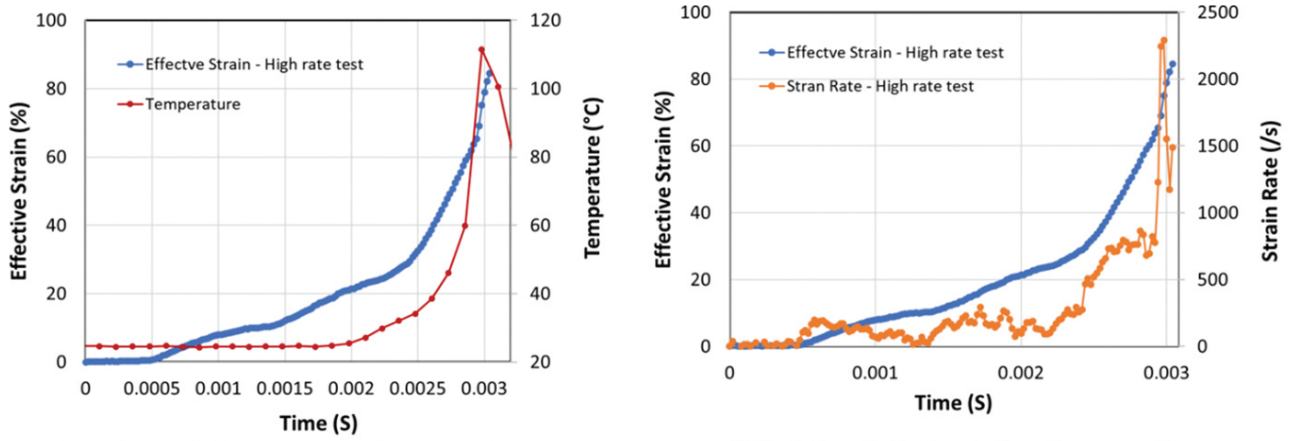

(a) Evolution of effective strain and corresponding temperature at the specimen center

(b) Evolution of effective strain and corresponding strain rate at the specimen center

Fig. 7 Evolution of temperature and strain rate during high-speed tensile testing of 5xxx-series aluminum at room temperature.

Results for cast aluminum.

Different with sheet aluminum, the cast aluminum demonstrates significantly reduced ductility. Figure 8 presents the evolution of effective strain and strain rate at the specimen center during a 3m/s high-speed test. In the initial stage (below 15% deformation), strain accumulates steadily while the strain rate maintains a plateau of approximately 300/s, accompanied by a minimal rise in temperature. Upon exceeding 15% strain, the strain rate increases rapidly to nearly 1000/s. Fracture occurs at approximately 20% strain with only moderate temperature increase. This high-rate fracture strain is virtually identical to the quasi-static result (0.1/s) as shown in Fig. 9, indicating that the ductility of this cast aluminum alloy is insensitive to strain rate.

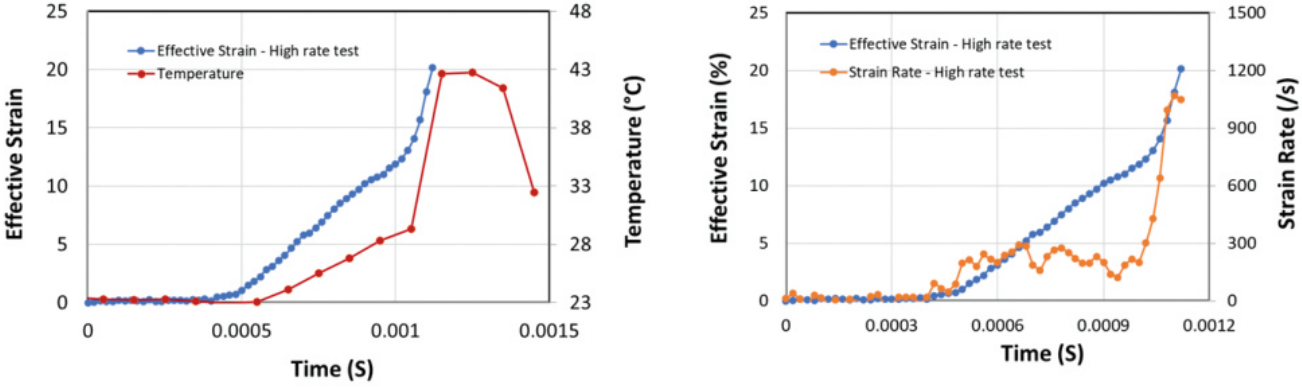

(a) Evolution of effective strain and corresponding temperature at the specimen center

(b) Evolution of effective strain and corresponding strain rate at the specimen center

Fig. 8 Evolution of temperature and strain rate during high-speed tensile testing of a cast aluminum material.

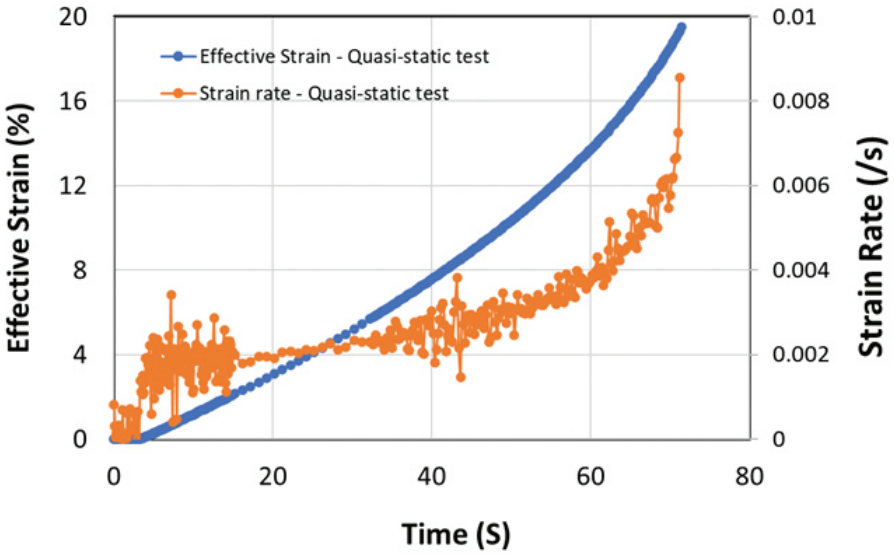

Fig. 9 Evolution of effective strain and strain rate during quasi-static tensile testing of a cast aluminum material.

Discussions

Figure 10 summarizes the comparison of localized fracture strain between quasi-static and high-speed tests for both the aluminum sheet and cast aluminum alloy. The contrasting fracture behaviors of the 5xxx-series sheet and the cast aluminum alloy highlight the critical influence of manufacturing processes on high-strain-rate performance.

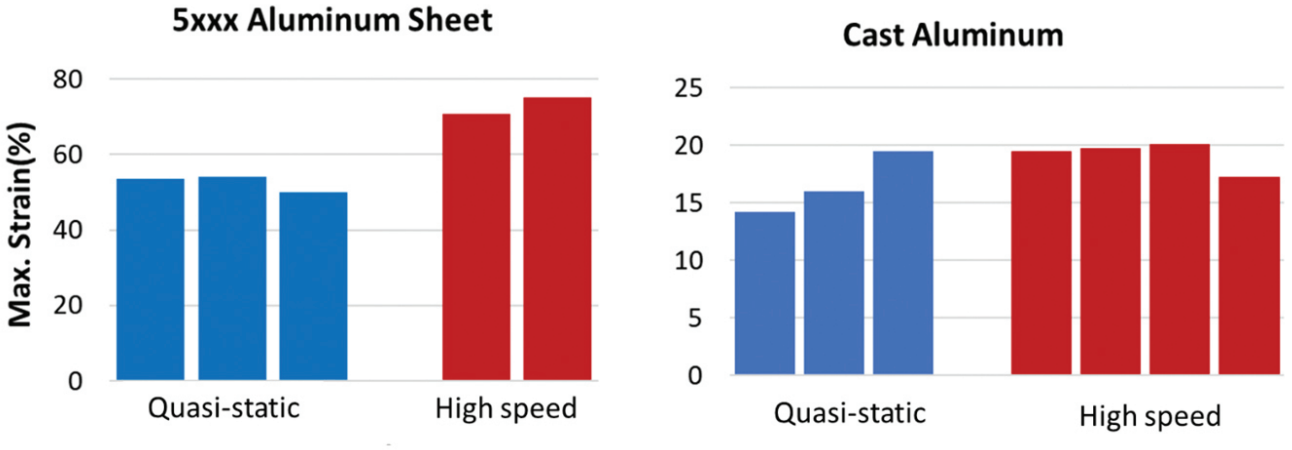

Fig. 10 Comparison of the fracture strain.

For the 5xxx-series sheet, the significant increase in fracture strain (from $50\%$to 75%) at high speed correlated directly with the observed temperature rise ($>100^{\circ}$C). This suggests that adiabatic heating induces thermal softening, which counteracts strain hardening and delays failure, effectively enhancing ductility under dynamic loading.

Conversely, the cast aluminum alloy displayed negligible strain-rate sensitivity, with fracture strains remaining consistent ($\sim 20\%$) across both quasi-static and dynamic regimes. The inherent lower ductility of the cast microstructure limits the accumulation of plastic work, thereby generating insufficient heat to trigger significant thermal softening before fracture occurs. Consequently, while high-speed deformation promotes enhanced ductility, cast components remain limited by their initial microstructural state and do not exhibit the same deformation-induced softening.

Summary and Future Works

This study established a robust experimental framework for characterizing the high-strain-rate fracture behavior of two automotive aluminum alloys by synchronizing high-speed DIC with high-speed IRT. By temporally aligning thermal fields with deformation contours, this methodology successfully decoupled the mechanical and thermal contributions to failure, providing a quantitative assessment of adiabatic heating effects.

The application of this coupled technique to 5xxx-series sheet and cast aluminum alloys revealed a distinct divergence in rate sensitivity driven by manufacturing processes. These findings challenge the conventional assumption that aluminum is purely rate-insensitive. Instead, they demonstrate that high-rate fracture is a competition between strain hardening and adiabatic thermal softening, a mechanism heavily dependent on the material's initial ductility and manufacturing process.

To further enhance the predictive accuracy of automotive crash simulations, future research will focus on the following areas:

- As the current study primarily focused on methodology development, future work will extend the testing envelope to include a broader range of strain rates and additional material compositions.
- The results from this study rely on high-speed tensile test data involving transient temperature rise. To isolate the thermal effect, quasi-static tensile tests will be conducted at constant elevated temperatures. Comparing isothermal behavior with transient high-speed data will validate the specific relationship between temperature and softening.
- While this study focused on uniaxial tension, automotive components undergo complex loading cases during a crash. Future testing will utilize the DIC-IRT setup to characterize fracture behavior under shear, plane-strain, and other loading paths to construct a comprehensive fracture loci.
- The experimental temperature-strain data obtained in this study will be used to calibrate and validate temperature-dependent material models such as GISSMO and modified Johnson-Cook. Incorporating the thermal softening parameters directly into FEA will improve the fidelity of crashworthiness simulations.

References

1. H. Yamada, T. Kami, R. Mori et al.: Strain rate dependence of material strength in AA5xxx series Aluminum alloys and evaluation of their constitutive equation, Metals 2018, 8, 576
2. Y. Chen, A. Clausen, O. Hopperstad et al.: Stress–strain behavior of aluminum alloys at a wide range of strain rates, International Journal of Solids and Structures 46 (2009) 3825–3835
3. P. Summers, Y. Chen, C. Rippe et al.: Overview of aluminum alloy mechanical properties during and after fires. Fire Sci Rev 4, 3 (2015). https://doi.org/10.1186/s40038-015-0007-5
4. Sutton, M. A., Orteu, J. J., & Schreier, H. (2009). Image correlation for shape, motion and deformation measurements. Springer Science & Business Media.
5. Pan, B., Qian, K., Xie, H., & Asundi, A. (2009). Two-dimensional digital image correlation for in-plane displacement and strain measurement: a review. Measurement science and technology, 20(6), 062001.
6. GOM GmbH. (2020). ARAMIS User Manual - Optical 3D Deformation Analysis.
7. Tyson, J., Schmidt, T., & Galanulis, K. (2002). Advanced photogrammetry for robust deformation and strain measurement. Proceedings of the SEM Annual Conference on Experimental and Applied Mechanics.
8. X. Xie, D. Zeng, J. Li, J. Dahl, Q. Zhao, L. Yang: Tensile test for polymer plastics with extreme large elongation using quad-camera digital image correlation, SAE 2016-01-0418
9. Gagnon, J. P., & Richards, A. (2013). High-speed infrared imaging for fast transient thermal analysis. Telops Inc.
10. Bjerke, T., & Lamberson, L. (2018). Dynamic thermodynamics of cracks in PMMA. Journal of the Mechanics and Physics of Solids, 117, 1-17.
11. Johnston, J. P., et al. (2018). High-speed infrared imaging of dynamic failure in polymers. Experimental Mechanics.
12. Bowers, S., Garbarino, T., Schmidt, T., Roselli, M., and Shremshock, M. Thermal strain correction of 3D image correlation data using infrared cameras – validation and example. Trilion and Telidyne Flir, iDICs (2022).
13. Maynadier, A., Poncelet, M., Lavernhe-Taillard, K., & Roux, S. (2012). One-shot measurement of thermal and kinematic fields: Infrared image correlation (IRIC). Experimental Mechanics, 52(3), 241-255.